Structural Integrity and Fracture, Dyskin, Hu & Sahouryeh (eds.)
© 2002 Swets & Zeitlinger, Lisse, ISBN 90 5809 513 4

Numerical analysis of thermally cycled Ball Grid Array solder joints

C. Yan[1], Q.H. Qin[1] and Y.-W. Mai[1, 2]
[1]*Centre of Advanced Materials Technology, School of Aerospace, Mechanical and Mechatronic Engineering J07, The University of Sydney, Australia.* [2]*Department of Manufacturing Engineering and Engineering Management, City University of Hong Kong, Kowloon Tong, Hong Kong*

ABSTRACT: Finite element analysis of a plastic ball grid array (PBGA) package with different solder alloys was carried out in a simulated thermal cycling loading. The results indicated that high constraint was associated with the joints closest to the edge of the silicon chip, especially for the 97.5Pb2.5Sn alloy. On the other hand, high inelastic strain was developed in the joints close to the package center for the 60Sn40Pb and 96.5Sn3.5Ag alloys.

1 INTRODUCTION

Ball Grid Array (BGA) has been increasingly used to replace the traditional Pin Grid Array (PGA) technique to further reduce the footprints and increase the packaging density. Recently, explosive growth in the development of this emerging technology has been devoted to Ceramic BGAs (CBGA), Plastic BGAs (PBGA), and Tape Automated Bonding BGAs (TBGA). As bismaleimide triazine (BT) resin is cheaper than ceramic substrate and has a lower dielectric constant, more attentions have been paid to the PBGA technology. For both flip chip and BGA technologies, the main interconnection technique is called Surface Mount Technology (SMT) in which solder joints are employed to connect chips and packages to substrate and printed circuit board (PCB). Because of the extreme mismatch in the coefficients of thermal expansion (CTE) between the silicon die, solder alloy and substrate materials, thermal-mechanical stress will be developed in a package during thermal cycling. Compared to traditional Through-Hole Technology (THT), the high packaging density and weak support from the foot area associated with SMT, especially in BGA method, make it more difficult to inspect and analyze the reliability of solder joints. Therefore, it is necessary to predict the potential failure sites in BGA packages for product design. To this end, a thorough understanding of stress-stain distributions in a PBGA assembly is essential. In this work, solder joints in a plastic ball grid array (PBGA) package are analyzed based on extensive finite element analysis with both temperature-dependent steady creep response and damage evolution.

2 NUMERICAL ANALYSIS

2.1 *Materials properties*

A typical PBGA package was analyzed and the dimension of the package is the same as that in Jung *et al.* (1997). The schematic showing the diagonal cross section view is shown in Figure 1(a).

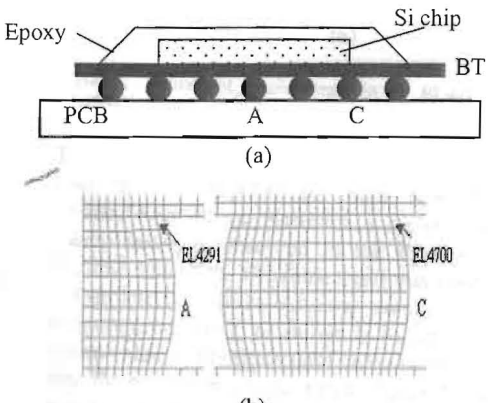

Figure 1. (a) Schematic of the PBGA assembly in diagonal direction, and (b) locations of elements 4291 and 4700 in the solder joints.

The silicon chip is mounted on a BT substrate and encapsulated with an epoxy molding compound. The substrate materials then were connected with the printed circuit board (PCB) with solder joints.

The ball diameter of the solder joint was 0.71mm with a height of 0.36mm. Three conventional solder alloys, 60Sn40Pb, 97.5Pb2.5Sn and 96.5Sn3.5Ag were analyzed. The material properties of the silicon chip, epoxy molding compound, substrate and solder alloys can be referred to work of Yan *et al.* (2001) & Lau (1995). Thermal load was applied to the package in terms of temperature cycles between -55°C and 125°C. The holding time was 0.25 h at both the high and low temperature shelves. The total loading time was 5 h.

2.2 *Finite element analysis*

In this study, isotropic thermoviscoplasticity is introduced for modeling the response of rate independent plastic and time dependent creep deformations. The multiaxial stress-strain relation is given by

$$\dot{\varepsilon}_{ij} = \dot{\varepsilon}_{ij}^{el} + \dot{\varepsilon}_{ij}^{pl} + \dot{\varepsilon}_{ij}^{cr} + \dot{\varepsilon}_{ij}^{th}, \qquad (1)$$

where the total strain rate tensor is the sum of the elastic, plastic, creep and thermal strain rate tensor, respectively. The hyperbolic sine law is used to relate the steady state creep rate to stress and temperature during thermal loading. This yields the creep strain rate tensor as

$$\dot{\varepsilon} = A[\sinh(B\sigma)]^n \exp(-\frac{\Delta H}{R}), \qquad (2)$$

where $\dot{\varepsilon}$ and σ are the uniaxial equivalent creep strain rate and equivalent deviatoric stress, respectively. A, B, n are material constants. ΔH and R are activation energy and universal gas constant, respectively. All material constants in Eq.2 are given in Lau (1995). Large deformation finite element analysis was carried out with finite element code ABAQUS (Version 6.2). The diagonal plane was modeled since the corner solder joint is most susceptible to fatigue failure (Jung *et al.*, 1997). Only one-half of the plane was modeled due to symmetry. Plane strain condition was assumed.

3 RESULTS AND DISCUSSION

The finite element simulations showed that at a given temperature high stress and strain are mainly observed in the element 4291 (EL4291) of the central joint in the package (joint A) and the element 4700 (EL4700) in the joint just under the edge of the silicon die (joint C), as shown in Figure 1(b). Therefore, the results for the above two elements were reported in this paper. Figure 2 gives the variation of equivalent plastic strain (PEEQ) for the EL4291 and EL4700 subjected to five cycles of the cyclic temperature load.

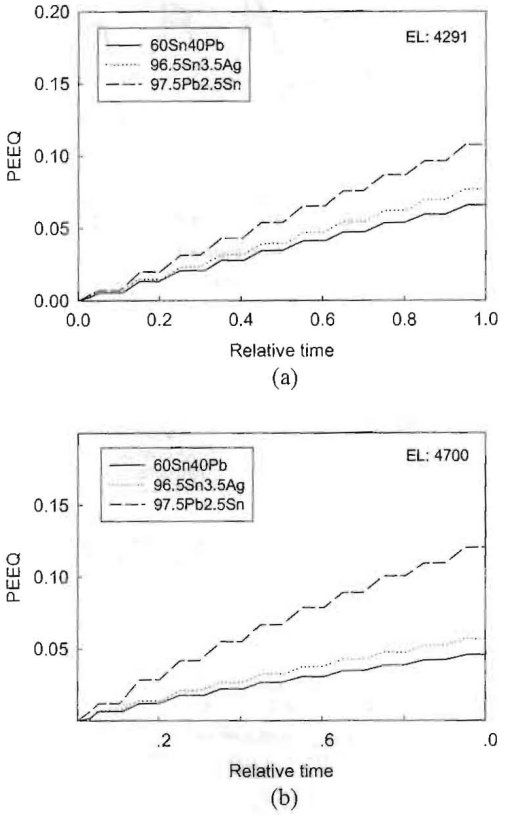

Figure 2. Equivalent plastic strain in (a) EL4291, and (b) EL4700.

The equivalent plastic strain in the EL4291 is higher than that in EL4700 for both 60Sn40Pb and 96.5Sn3.5Ag alloys. However, a higher equivalent plastic strain is observed in the EL4700 for the 97.5Pb2.5Sn alloy. The same trend was observed for the variation of equivalent creep strain (CEEQ) with temperature cycling, as shown in Figure 3. The absolute value of the equivalent creep strain is smaller than the equivalent plastic strain. Figure 4 shows the variation of shear stress (σ_{12}) with the temperature cycling, where σ_o is the yield stress. A very similar shear stress distribution can be observed in both the EL4291 and EL4700. In other words, the shear stress distribution seems not sensitive to the locations in the package. Figure 5 shows the variation of opening stress (normal to the PCB) with the thermal cycling. A higher opening stress is associated with the El4700, which is located

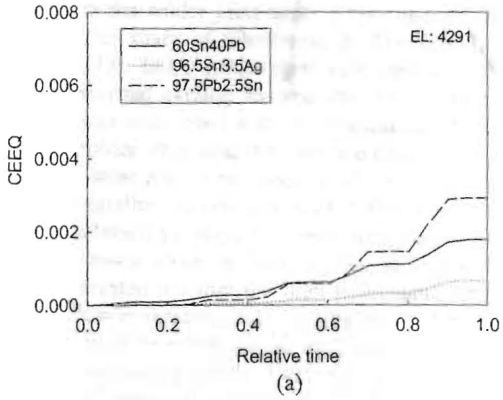

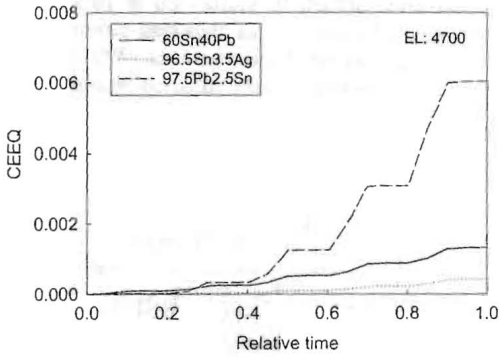

Figure 3. Equivalent creep strain in (a) EL4291, and (b) EL4700.

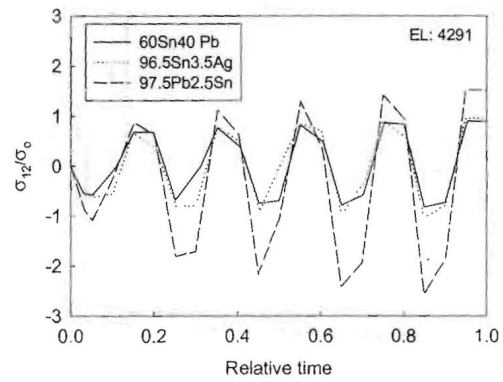

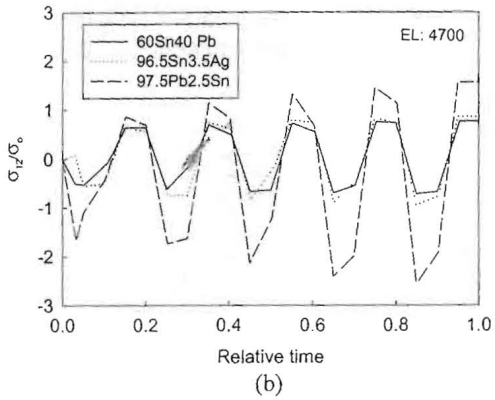

Figure 4. Shear stress in (a) EL4291, and (b) EL4700.

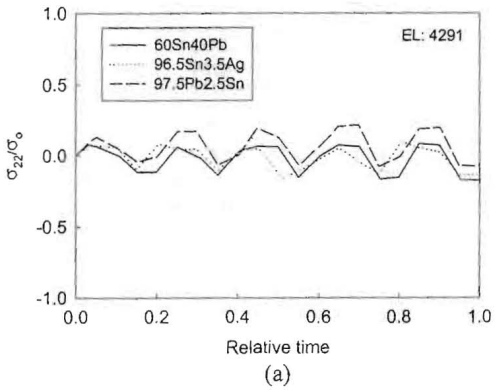

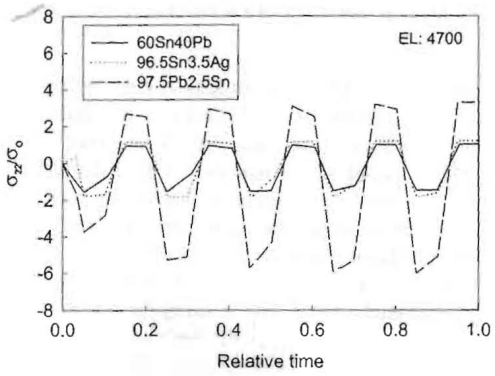

Figure 5. Opening stress in (a) EL4291, and (b) EL4700.

in the solder joint near to the edge of silicon chip. The study of Ghaffarian & Kim (2000) on 63Sn-37Pb BGA solder joint subjected to –55°C-125°C thermal cycling showed that the failure mechanism was associated with the nucleation of voids in the solder alloy near the interface between substrate and solder joint. Our recent work on ductile fracture of metallic materials indicated that constraint (stress triaxiality) played a very important role in void growth (Yan & Mai, 1998). Huang *et al* (1996) pointed out that the high hydrostatic tension stress due to constraint and thermal mismatch and voiding could be identified as the failure mechanism in an electronic package. The rapid nucleation and growth of voids was called cavitation instability and it could lead to the failure of ductile components in electronic packages such as metallization. Huang *et al* (1996) also estimated the cavitation stress for an elastic-perfectly plastic solid as

$$\frac{\sigma_{cavitation}}{\sigma_o} = \frac{2}{3}\left\{1 - \frac{\sqrt{1+4\eta}-1}{2\eta} + \ln\frac{2E}{3\sigma_o} + \ln\frac{\exp[(\sqrt{1+4\eta}-1)\frac{V_f}{2}]-1}{\exp[\sqrt{1+4\eta}-1)\frac{V_f}{2}]-1+V_f}\right\}, \quad (3)$$

where $\eta = 3\sigma_o/(2EV_f)$. E and V_f are Young's modulus and initial void volume fraction, respectively. Figure 6 shows the variation of cavitation stress with the initial void volume fraction.

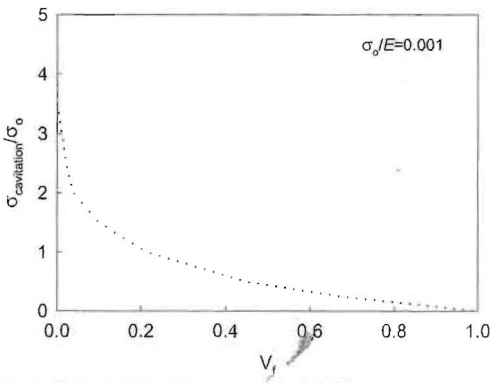

Figure 6. Cavitation stress versus the initial void volume fraction.

The cavitation stress decreases rapidly with increase of void volume fraction. Huang *et al* (1996) also shown that yield stress and hardening exponent had a little effect on the cavitation stress. Figure 7 gives the variation of stress triaxiality (σ_m/σ_o) for the EL4291 and EL4700 subjected to five cycles of the cyclic temperature load.

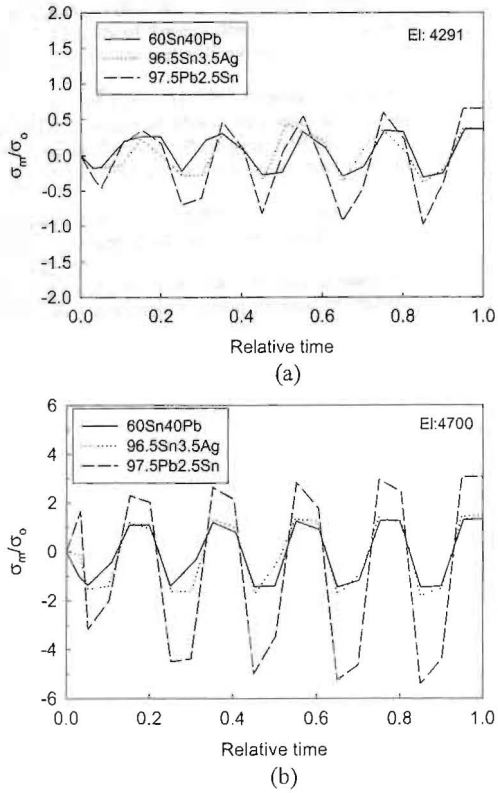

Figure 7. Evolution of stress triaxiality in (a) EL4291, and (b) EL4700.

The stress triaxiality in the EL4700 is much higher than that in EL4291 for all solder alloys. The stress triaxiality in the joint with 97.5Pb2.5Sn alloy is much higher than that in the joints with 60Sn40Pb and 96.5Sn3.5Ag alloys. In a first approximation, the stress triaxiality developed in the EL4700 with 97.5Pb2.5Sn solder alloy is already comparable to the cavitation stress even at very low void volume fraction (Figures 6 and 7(b)). Therefore, failure is expected to start from the solder joint close to the edge of silicon slip due to the higher stress triaxiality. Also, cavitation instability is much easier to occur in the 97.5Pb2.5Sn alloy as compared to 60Sn40Pb and 96.5Sn3.5Ag. Further experimental investigation on the failure mechanism of solder joints in BGA packages is needed.

4 CONCLUSIONS

In this study, finite element analyses were carried out for a PBGA package with different solder alloys. The results indicated that high inelastic strain (plastic and creep) was developed in the joints close to the package center for the 60Sn40Pb and 96.5Sn3.5Ag alloys. However, high opening stress and stress triaxiality were associated with the joint closest to the edge of the silicon chip for all three alloys studied. The stress triaxiality in the joint with 97.5Pb2.5Sn alloy was much higher than that in the joints with 60Sn40Pb and 96.5Sn3.5Ag alloys.

ACKNOWLEDGEMENT

The authors wish to thank the Australian Research Council (ARC) for the support of this project. C. Yan is also supported by a Sydney University Sesqui Fellowship.

REFERENCES

Ghaffarian, R and Kim, N.P. 2000. Reliability and failure analyses of thermally cycled ball grid array assemblies. *IEEE Trans, CPT.* 23: 528.

Huang, Y., Hu, K.X., Yeh, C.P., Li, N.Y. and Hwang, K.C. 1996. A model study of thermal stress-induced voiding in electronic packages. *Journal of Electronic Packaging* 118: 229.

Jung, W., Lau, J.H. and Pao, Y.H. 1997. Nonlinear analysis of full-matrix and perimeter plastic ball grid array solder joints. *Journal of Electronic Packaging* 119: 163.

Lau, J.H. 1995. *Ball Grid Array Technology.* McGraw-Hill: New York.

Yan, C. and Mai, Y.W. 1998. Effect of constraint on void growth near a blunt crack tip. *International Journal of Fracture* 92: 287.

Yan, C., Qin, Q.H. and Mai, Y.W. 2001. Nonlinear analysis of plastic ball grid array solder joints, *Journal of Materials Science: Materials in Electronics* 12: 667.